Calcif Tissue Int (2002) 72:197–205
DOI: 10.1007/s00223-002-1025-6

Calcified Tissue International

Laboratory Investigations

The Integrin $\alpha_v\beta_3$ and CD44 Regulate the Actions of Osteopontin on Osteoclast Motility

M. A. Chellaiah,[1] K. A. Hruska[2]

[1]Department of Oral & Craniofacial Biological Sciences, University of Maryland, Baltimore, MD 21201, USA
[2]Department of Pediatrics, Washington University School of Medicine, St. Louis, MO 63110, USA

Received: 13 March 2002 / Accepted: 26 July 2002 / Online publication: 10 December 2002

Abstract. In the studies reported here we demonstrate that osteopontin is secreted from the basolateral surfaces of osteoclasts where it binds to the $\alpha_v\beta_3$-integrin, suggesting that it may be an autocrine factor. Osteopontin stimulation of osteoclasts produced changes in cell shape by causing disruption of peripheral podosome structures and formation of actin filaments at the leading edge of the migrating osteoclasts. The latter was part of the assumption of a motile phenotype prior to cells reforming peripheral ring type podosome containing clear zones. It is well established in our laboratory as well as in others that osteopontin stimulated osteoclast motility and bone resorption. The effect of osteopontin was mimicked by RGD containing peptides and blocked by a $\alpha_v\beta_3$ antibody, demonstrating that signals generated by integrin ligation contributed to the actions of osteopontin. In addition, the migratory effects of osteopontin on osteoclasts were also mediated through CD44 receptors since blocking antibodies to CD44 blocked stimulation of motility. Our data strongly suggest that osteopontin is an osteoclast autocrine motility factor binding to $\alpha_v\beta_3$ and CD44 during stimulation of osteoclast migration.

Key words: Osteoclasts — Osteopontin — Integrin $\alpha_v\beta_3$ — CD44 — Motility

Osteoclasts are multinucleated giant cells with bone-resorbing activity. Bone resorption appears to proceed by the intricate coordination of the processes of attachment to bone, polarized secretion of acid and proteases, and active motility of osteoclasts along the bone surface [1–3]. As osteoclasts crawl over bone surfaces they require rapid attachment and release from the extracellular matrix [4–6]. The adhesion structures, podosomes, are uniquely designed for this purpose. After osteoclasts attach to the bone surface, podosomes develop highly polarized cytoplasmic organization in their ruffled borders and clear zones. The clear zone, which surrounds the ruffled border, seals the extracellular resorbing compartment in which bone resorption takes place [7]. Actin rings in the clear zone represent specialized mechanisms of adherence to bone surfaces during resorption.

The adhesion of osteoclasts through podosomes involves interaction of cell surface receptors, integrins, especially $\alpha_v\beta_3^a$, with extracellular bone matrix proteins. Osteoclast $\alpha_v\beta_3$ recognizes several bone matrix proteins containing the Arg-Gly-Asp (RGD) sequence, osteopontin (OPN), bone sialoprotein (BSP), and vitronectin (VN) [8–10]. Osteopontin, an RGD-containing bone matrix protein [11–13] plays a key role in anchoring osteoclasts to bone surface. A large quantity of osteopontin secretion by osteoclasts [14] suggests additional roles for OPN besides its function as an anchorage protein. We have demonstrated that OPN, as a soluble protein, stimulates signal transduction in osteoclasts, including activation of c-src and phosphatidylinositol 3-hydroxyl kinase (PI3-kinase) [15, 16]. OPN binding to integrin $\alpha_v\beta_3$ in osteoclasts stimulates gelsolin-associated phosphatidylinositol kinases, leading to increased levels of gelsolin-associated polyphosphoinositides such as PtdIns 4,5-P_2, PtdIns 3,4-P_2 and PtdIns 3,4,5-P_3; uncapping of actin barbed ends, stimulation of actin polymerization, and an increase in F-actin levels [15]. OPN binding to the $\alpha_v\beta_3$ integrin of osteoclast podosomes stimulated cytoskeletal reorganization and bone resorption by activating a heteromultimeric signaling complex, which includes gelsolin, src, and PI3-kinase [17, 18].

The interaction of OPN with the $\alpha_v\beta_3$ integrin through its RGD domain has been widely studied in cell adhesion [8–11] but the OPN domains involved in chemotaxis are less well defined. They may also involve the RGD sequences since cell movement involves an organized process of detachment from the matrix and reattachment [19]. According to the report by Weber et al.

Correspondence to: M. A. Chellaiah; E-mail: mac001@dental.umaryland.edu

[20], OPN, which is a ubiquitous extracellular matrix glycoprotein, may be another ligand for CD44. CD44 has also been implicated in chemotaxis mediated by OPN [20], as well as in bone resorption [21].

The objective of the studies herein was to investigate the changes in the localization of $\alpha_v\beta_3$ integrin and actin in the cycle of osteoclast adhesion, detachment, and migration in response to OPN. These studies indicate that OPN stimulated formation of lamellipodia-like extensions at the leading edge of cells, with the formation of new adhesion structures and the disruption of the actin-enriched podosomes at the trailing end. This leads to a long dendritic-like morphology, which is a motile phenotype. The new adhesion structures demonstrate colocalization of actin and $\alpha_v\beta_3$. As osteoclast, podosomes in the clear zone detach from the matrix and the original attachment points containing $\alpha_v\beta_3$/actin were left behind. We have demonstrated that OPN is secreted from the basolateral surface of avian osteoclast precursors and it colocalizes with integrin $\alpha_v\beta_3$ at the basolateral and clear zone surfaces. Our studies indicate that OPN-induced cell migration requires both $\alpha_v\beta_3$ and CD44 receptors.

Materials and Methods

Rhodamine phalloidin was obtained from Molecular Probes (Eugene, OR). Anti-CD44 antibodies to the standard CD44 (monoclonal and polyclonal) were purchased from BioSource International Inc. (Camarillo, CA) and Santacruz Biotechnology (Santacruz, CA). Transwell chamber was purchased from Corning Inc. Costar (Corning, NY). CY2 or CY3 conjugated anti-mouse or rabbit antibodies were purchased from Jackson Immunoresearch laboratories, Inc. (Westgrove, PA). GRGDS peptide was purchased from Gibco-BRL (Gaithersberg, MD). All the other chemicals including hyaluronic acid were purchased from Sigma Chemicals (St. Louis, MO).

Preparation of Osteoclasts

Avian osteoclast precursors were prepared as previously described [15]. Briefly, osteoclast precursors were isolated from bone marrow of egg-laying hens, maintained on Ca^{2+}-deficient diets. Partially purified preparations of mononuclear cells were recovered from the interface of Ficoll/Hypaque gradients as described. Nonadherent cells were separated from the adherent population after 18–24 hours in culture. The nonadherent cells were sedimented, resuspended in fresh media (5×10^6cells/ml), and cultured in the presence of cytosine arabinoside (5 μg/ml). Multinucleated osteoclast precursor cells formed between 3 and 6 days in culture. The multinucleated cell preparations were uniformly TRAP-positive, and resorbed bone by forming resorption pits on dentine slices.

Actin Staining. Osteoclasts were rinsed briefly with PBS containing 5 mM EGTA (PBS-EGTA) and fixed in 4% (w/v) paraformaldehyde in PBS-EGTA for 20 min at 37°C. Coverslips were immersed in 47.5% ethanol containing 5 mM EGTA for 15 min at room temperature and rinsed with several changes of PBS-EGTA. The coverslips were then stained with 1:20 dilution of rhodamine phalloidin in PBS-EGTA for 30 min at 37°C [17]. After rinsing several times with PBS-EGTA, coverslips were mounted on a mounting solution (Vector Laboratories, Inc., Burlingham, CA). Rhodamine phalloidin images were recorded on a Zeiss LSM 410 confocal laser-scanning microscope (Thornwood, NY). Confocal images were processed by using the Adobe Photoshop software program (Adobe Systems, Inc., Mountain View, CA).

Immunostaining. Osteoclasts were cultured on glass coverslips or whale dentine slices. After 4 days in culture, cells were incubated with antibodies to $\alpha_v\beta_3$ and OPN as described previously [17]. Briefly, cells were fixed with 3% paraformaldehyde and permeablized with 10 mM Tris-HCl, pH 7.4, 150 mM NaCl, and 1 mM $CaCl_2$ containing 0.1% Triton X-100 for 1 min. The cells were washed and incubated with antibodies to $\alpha_v\beta_3$ and OPN (1:100 dilution) for 2 hours, washed, and counter-stained with fluorescein isothiocyanate-conjugated goat anti-mouse IgG. Actin staining of the cells stained for $\alpha_v\beta_3$ was performed using rhodamine phalloidin (1:20 dilution) as described above. The cells were washed and mounted on a slide in a mounting solution (Vector laboratories, Inc., Burlingham, CA) and viewed on a Zeiss LSM 410 confocal laser-scanning microscope (Thornwood, NY), and photomicrographs were developed [22]. CY2 and CY3 images were recorded using the 488 nm and 568 argon excitation lines, respectively. CY2 and CY3-labeled proteins were imaged with dual fluorescence [23]. The background (dentine) is shown in red (pseudocolor) by the reflected light (Figs. 3, 4, 5). Images were stored in TIF image format and processed by the Adobe Photoshop software program (Adobe Systems, Inc., Mountain View, CA).

Cell Migration Assays. Phagokinesis assays were performed in 6-well tissue culture dishes as described [23]. Osteoclasts were removed gently from the plate and seeded at a low density (1×10^5 cells per well). Some cells were treated with antibodies to the $\alpha_v\beta_3$ integrin (LM609) for 30 min prior to plating the cells on the colloidal gold surface. Once the cells were attached to the wells, substrates such as OPN or GRGDS were added to a final concentration of 10 μg/ml or 50 μg/ml, respectively. The cells migrated on this substrate, and phagocytized the gold particle to produce a white track free of the particle in a time-dependent manner. The migrating cells were visible as a black body [24]. The motility of the cell is evaluated by measuring the areas free of gold particles represented as areas moved in mm^2. The areas were measured by using a grided reticle in the eyepiece of a Nikon microscope using a 10× objective. (20–25 Tracks per experiment) were measured and three separate osteoclast preparations were used. PBS-treated cells served as control. Statistical comparisons were performed by analysis of variance (ANOVA) with the Bonferroni corrections (Instat for IBM, version 2.0; Graphpad software) as described below.

Transwell Migration Assay. Transwell migration chambers (Costar; 8-μm pore size) were used to assay chemotactic migration. Undersides of the membranes were coated with vitrogen 100 (collagen type 1) (30 mg/ml) at room temperature for 2 hours as directed by the manufacturer's instructions. Osteoclasts isolated as described above were pelleted and resuspended in α-MEM medium containing 1% serum and 2% BSA (50,000 cells/ml). Cells were added to the upper chamber in the above-mentioned medium (100 μl) and the indicated substrates (Fig. 7) were added to the lower chamber in α-MEM medium containing 1% serum and 2% BSA (600 μl). The concentrations of the substrates are as follows: OPN or VN 25 μg/ml; GRGDS 50 μg/ml; or hyaluronic acid 100 μg/ml. Some cells were pretreated with antibodies to the $\alpha_v\beta_3$ integrin (LM609) or OPN or CD44 to a final concentration of 50 μg/ml for 30 min prior to plating cells. Cell migration was allowed to proceed at 37°C in a standard tissue culture incubator for 12–14 hours. Cells that migrated to the undersides were stained, visualized, and counted as described [23]. Data are presented as the number of cells migrated (mean ± SEM) and all assays were performed in quadruplicates. Statistical significance was calculated as mentioned below.

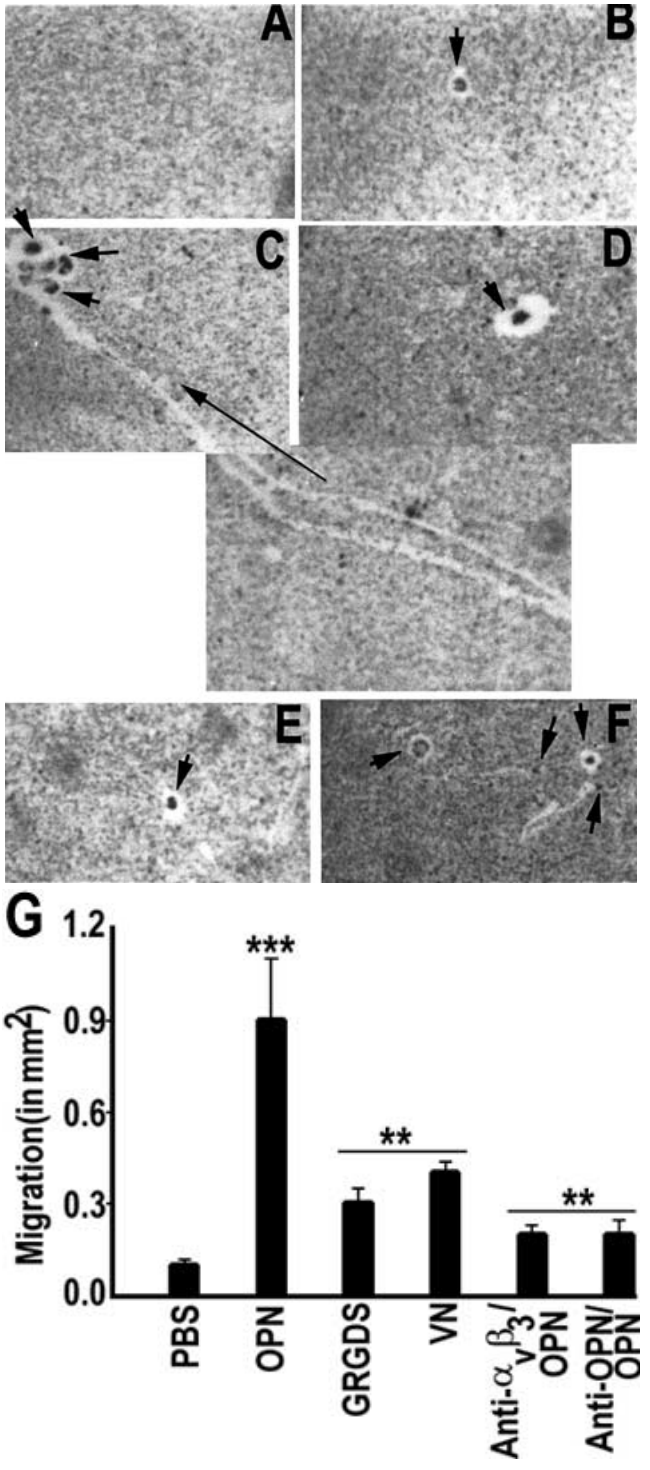

Fig. 1. Phagokinesis assay-effect of OPN on the motility of osteoclasts. Osteoclasts motility was assessed by phagokinesis assay *in vitro*. After osteoclasts were attached to the coverslips, the following test substances were added: B-PBS, C-OPN, D-GRGDS, E-anti-OPN/OPN, F-anti-$\alpha_v\beta_3$/OPN. (**A**) Colloidalgold particles only (no cell added). All the photographs are taken at the same magnification (×100 in the lower-power view). The area of the track is seen free of the gold particles. Cells werevisible inside the white track as a black body. Results are representative of three separate experiments. (**G**) The motility of the cell is evaluated by measuring the areasfree of gold particles, represented as areas moved in mm^2. Results shown are mean ± SEM of three independent experiments. ***P0.0001-PBS, GRGDS, and VN vs OPN; **P0.001-VN and GRGDS vs PBS; **P0.001-anti-$\alpha_v\beta_3$/OPN or anti-OPN/OPN vs OPN.

Data Analysis

All comparisons were made as "% control" which refers to vehicle-treated cells. The other treatment groups in each experiment were normalized to each control value. Data presented are mean ± SEM of experiments done at different times normalized to intra-experimental control values. Analysis of variance (ANOVA) was used for statistical comparisons, with the Bonferroni corrections (Instat for IBM, version 2.0; Graphpad software).

Results

Osteoclast Response to Added Osteopontin

To examine the actions of OPN on motility we performed phagokinesis assays demonstrating cell movement related to phagocytosis. Phagokinesis assays estimate motility by measuring cell tracks formed by phagocytosis of colloidal gold particles by migrating cells [25]. Osteoclasts plated on colloidal gold chloride coated cover slips were phagocytic as shown by the accumulation of gold particles in the cells (Fig. 1). Both recombinant OPN and GRGDS stimulated movement of osteoclasts (Figs. 1C, D). Osteoclasts treated with OPN exhibited higher rates of motility compared to GRGDS-treated cells. GRGDS-treated osteoclasts cleared areas of gold chloride around the cell (Fig. 1D) whereas OPN-treated osteoclasts moved in a specific direction (Fig. 1C). The representative studies shown in Figure 1 were reproduced three times with cells isolated from three different chickens (Fig. 1G). An anti-$\alpha_v\beta_3$ antibody (LM609) was used to verify the role of integrin $\alpha_v\beta_3$ in OPN-mediated migration. OPN induced osteoclast motility was inhibited by either anti-OPN (Figs. 1E, G) or anti-$\alpha_v\beta_3$ (Figs. 1F, G) antibodies. Basal levels of migration were observed in cells treated with the antibodies (Figs. 1E, F) and OPN. The data were the compiled results from three separate osteoclast preparations and each experiment was a mean of 15–25 cell tracks. Significantly greater osteoclast motility was observed in OPN-treated osteoclasts compared with GRGDS or VN-treated cells (Fig. 1G).

Analysis of Distribution of Actin in Osteoclasts Subjected to Phagokinetic Movement

Osteoclasts subjected to phagokinetic migration assays on glass coverslips were fixed and stained for actin using rhodamine phalloidin. Resting and OPN-treated osteoclasts are shown in Figure 2. The changes in actin organization in larger (A and B) and smaller (A′ and B′)

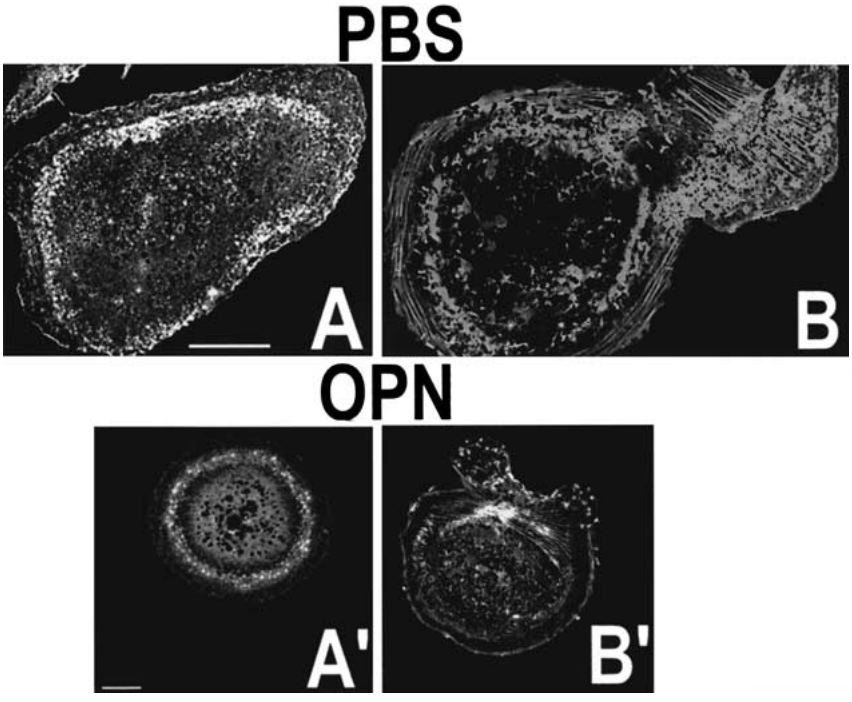

Fig. 2. Actin distribution in osteoclasts subjected to motility. Osteoclasts subjected to phagokinetic migration on coverslips were fixed and stained with rhodamine phalloidin. The treatments are A and A′-PBS; B and B′-OPN. Accumulation of gold particles (black spots) was more inside the cells treated with OPN (B & B′) than the osteoclasts treated with PBS (A and A′). Two different sizes of osteoclasts are shown. Scale bar A and B 100 μm; A′ and B′ 25 μm.

osteoclasts are shown (Bar: A and B 100 μM; A′ and B′ 25 μm). Similar to previous observations [17, 26], osteoclasts treated with PBS demonstrated peripheral dot-like podosome structures. Even though the osteoclast shown in Figure A demonstrates an elongated motile cell shape, the peripheral podosome structures are still intact. In the presence of OPN, osteoclasts exhibited lamellipodia-like structures at the leading edge (Fig. 2B and B′). The leading edge of the osteoclasts consisted of stress fibers and newly formed podosome-like structures enriched in F-actin (B and B′). Podosomes disruption was observed at the retractile end of osteoclasts (B and B′). Motile osteoclasts on dentine slices also demonstrated a 'dendritic' morphology with tapering rear end (Fig. 3).

Distribution of $\alpha_v\beta_3$ Integrin and Actin in Migrating and Resorbing Osteoclasts

Integrins not only provide highly stabilized adhesion and spreading, but are also involved in migration and cytoskeletal reorganization [27–29]. Since OPN stimulated the osteoclasts to undergo changes in cell shape [17, 26], we examined the distribution of the OPN receptor, $\alpha_v\beta_3$ integrin, in avian osteoclasts plated on dentine slices. These osteoclasts were costained with rhodamine phalloidin to analyze the actin distribution. Migrating osteoclasts exhibited a motile phenotype with a dendritic morphology. Integrin $\alpha_v\beta_3$ (Green) was localized diffusely over the plasma membrane of osteoclasts and was colocalized with actin (Red) (Fig. 3A). Colocalization of actin and $\alpha_v\beta_3$ integrin is seen in yellow color. The XZ scan of the osteoclast in A (Fig. 3B) demonstrated colocalization of $\alpha_v\beta_3$ and actin in the cellular projection, the attachment zones (indicated by white arrows), and in the basolateral surface. XZ scan of another osteoclast is shown in Figure 3C. Areas of $\alpha_v\beta_3$ and actin co-localization were present in the attachment zones (Fig. 3C, yellow pseudocolor), but areas of $\alpha_v\beta_3$ expression independent of actin were also present over the cell membrane (green in Fig. 3B and C). Similarly, areas of actin expression independent of $\alpha_v\beta_3$ were also present at the leading edge and in the lamellipodia-like extensions (Fig. 3A, indicated by arrowheads).

Resorbing osteoclasts attached to dentine revealed a more peripheral distribution of $\alpha_v\beta_3$ where it was strongly co-localized with actin (Fig. 4). By serial cross-sections, we have identified superficial resorption pits in the areas evacuated by osteoclasts (data not shown). Resorption pits, which had been evacuated by osteoclasts (indicated by white arrow), demonstrate colocalization of actin and integrin $\alpha_v\beta_3$ at the left behind attachment sites.

Distribution of OPN and $\alpha_v\beta_3$ in Osteoclasts Plated on Dentine Slices

In order to demonstrate the localization of OPN and $\alpha_v\beta_3$, the osteoclasts on dentine slices were immunostained with anti-$\alpha_v\beta_3$ (green) and anti-OPN (red) antibodies. Colocalization of OPN and $\alpha_v\beta_3$ was seen at the periphery and in the resorbing areas in yellow color. Cross-sections of osteoclast at 6 (**A**), 9 (**B**), and 12 (**C**) μm are shown in Figure 5. Colocalization of $\alpha_v\beta_3$ (green) was greater at 6 μm and only $\alpha_v\beta_3$ staining was seen at

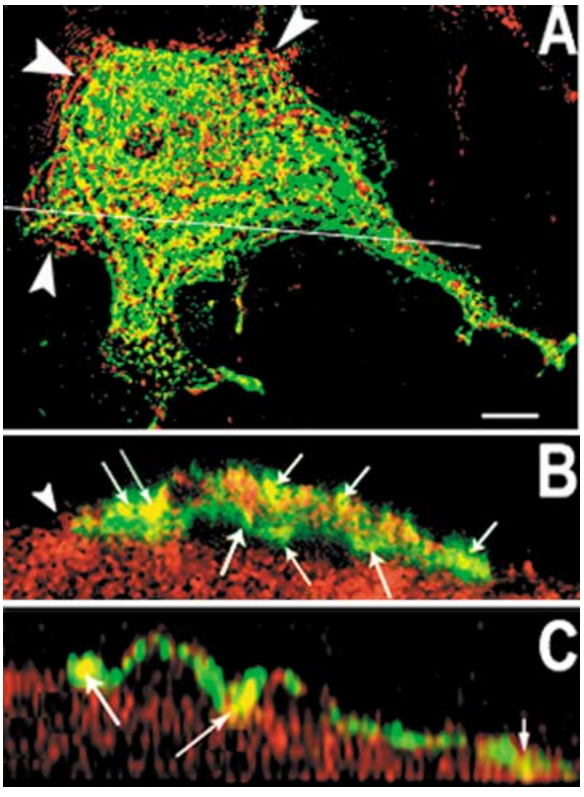

Fig. 3. Distribution of $\alpha_v\beta_3$ in migrating osteoclasts. Confocal microscopy of a motile osteoclast stained for integrin $\alpha_v\beta_3$ (green) and actin (red) is shown. (**A**) Integrin $\alpha_v\beta_3$ (green) was localized diffusely overthe plasma membrane of osteoclasts and was colocalized with actin (red) in some areas. Colocalization of actin and $\alpha_v\beta_3$ integrin is seen in yellow. (**B**) The XZ scan of the cell shown in Figure A. B & C-XZ scan of two different osteoclasts demonstrating colocalization (yellow) of actin and $\alpha_v\beta_3$ at the adhesion sites (white arrows) as well as at the basolateral surface. Diffuse staining of actin (red) or $\alpha_v\beta_3$ (green) is seen in some areas. The dentine is shown in red (pseudocolor) by the reflected light. Scale bar 25 μm.

9 μm cross-section, which is closer to the dentine surface. Colocalization of $\alpha_v\beta_3$ and OPN was seen as a ring-like structure in the resorbing areas (indicated by white arrows in Fig. 5A). The arrows in Figures A and C point to the areas containing resorption pit and these pits are very shallow (Fig. 5C). Recent observations in mouse osteoclasts with deeper resorption pits demonstrated that OPN is secreted both at basolateral and ruffled border surfaces. The OPN, which is secreted by osteoclast, is deposited on dentine [30]. When OPN expression was analyzed in avian osteoclasts plated on dentine slices, OPN was localized to the basolateral surface of the cell and in the peripheral attachment zone (Fig. 6A). As shown in Figure 6B, the YZ (right) and XZ (left) scans of the cell in 6A confirmed the basolateral surface

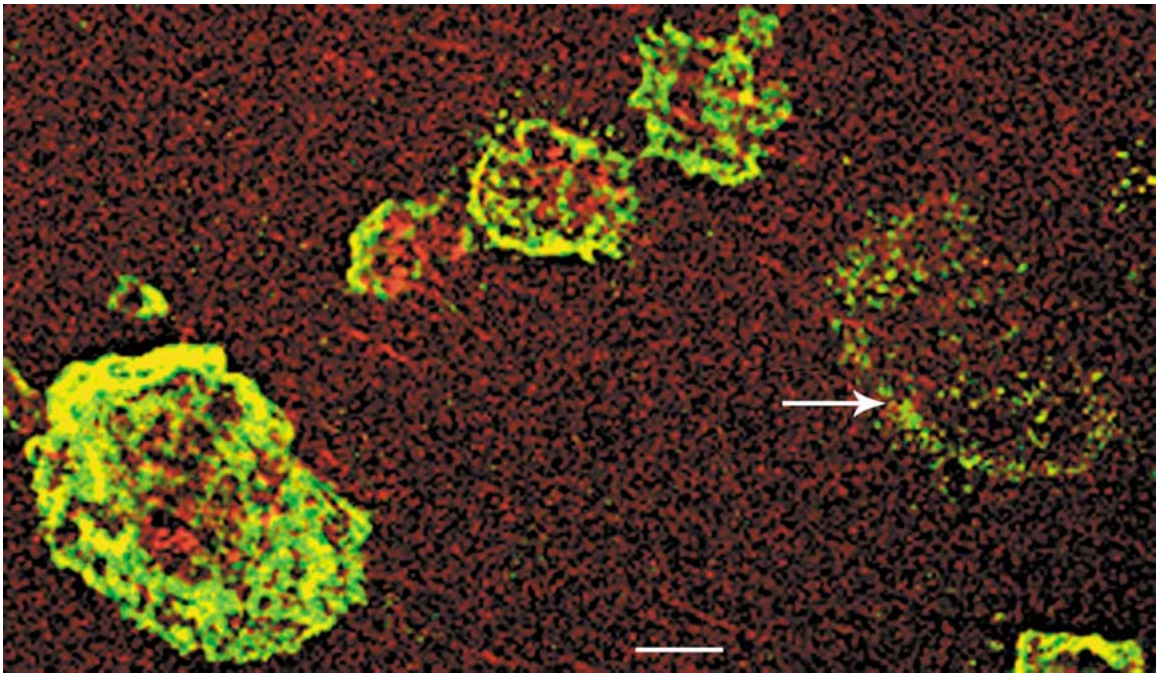

Fig. 4. Distribution of $\alpha_v\beta_3$ integrin and actin in the osteoclasts on dentine slice. Osteoclasts attached to dentine slices showed more peripheral distribution of $\alpha_v\beta_3$ (green) where it was strongly co-localized with actin (red). Colocalization (yellow) of $\alpha_v\beta_3$ and actin was seen in numerous dot-like structures in an evacuated resorption pit (white arrow). Staining of these resorption pits for OPN produced negative results. The dentine is shown in red (pseudocolor) by the reflected light. Scale bar 25 μm.

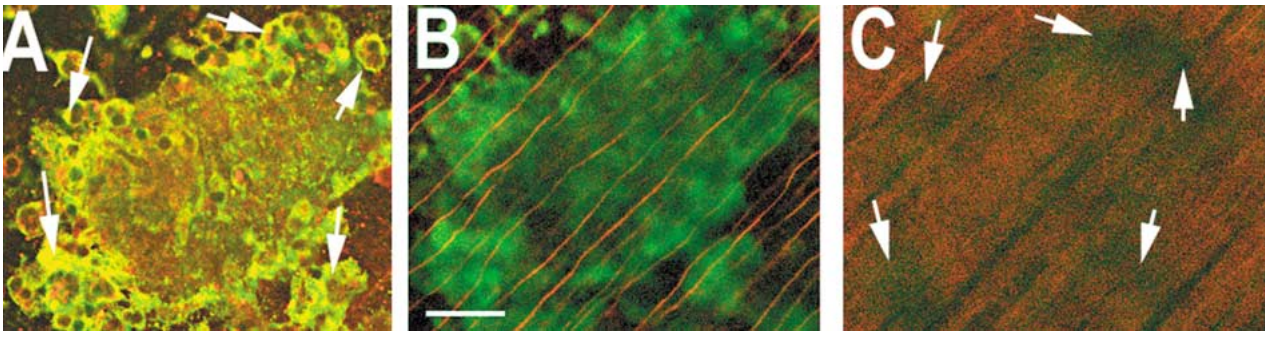

Fig. 5. Localization of OPN and $\alpha_v\beta_3$ in resorbing osteoclasts. Serial confocal microscopic sections of avian osteoclast precursors placed on dentine slices were taken beginning 6 μm and progressing through the cell to the dentine surface. 6 μm (**A**), 9 μm (**B**), 12 μm (**C**) sections are shown. Colocalization (yellow) of OPN (red) and $\alpha_v\beta_3$ (green) was seen at the periphery. The colocalizaton is more in the resorbing area (white arrows) in (**A**). White arrows in (**C**) point to the resorbed areas on the dentine slice. The dentine is shown in red (pseudocolor) by the reflected light. Scale bar 25 μm.

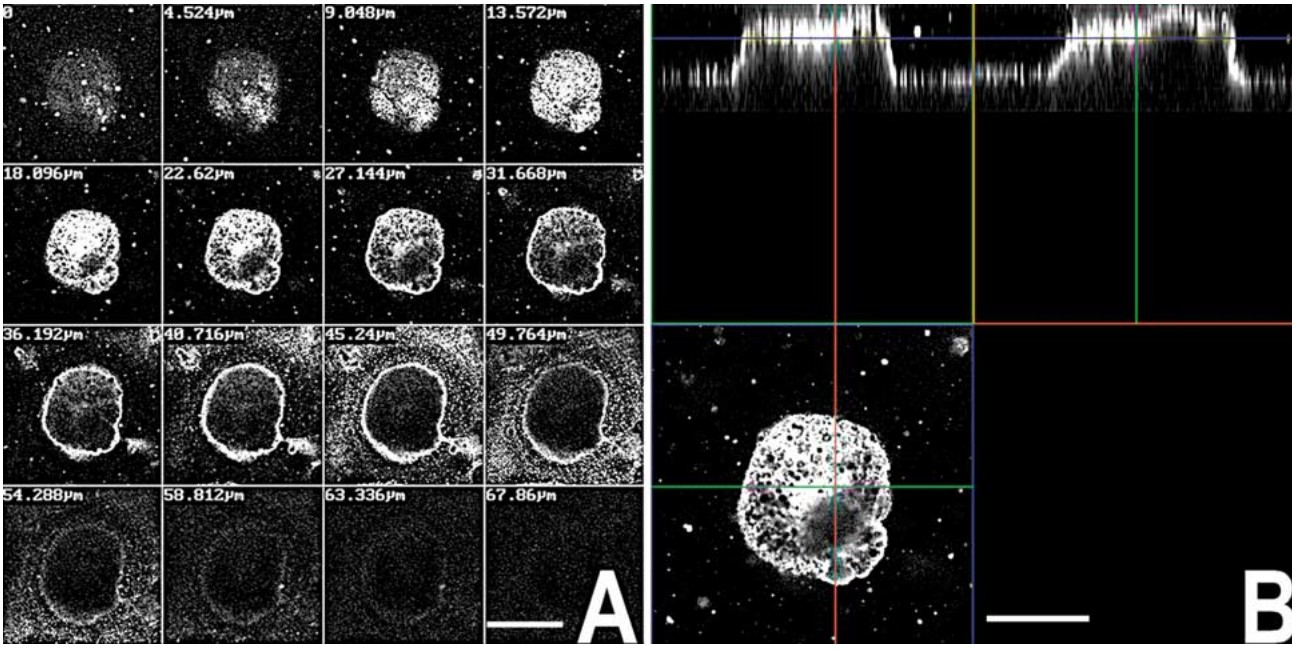

Fig. 6. Confocal microscopy of OPN expression in avian osteoclasts on dentine slices. (**A**) As shown in the array, OPN was expressed on the basolateral surface of the celland at the cell periphery as the surface of the dentine slice was approached. There was no staining of the ruffled membrane at the level of the resorption pit or of the dentine slice under the resorption pit. (**B**) The XZ and YZ scans both demonstrated clear distribution of OPN at the basolateral surface. These results were reproduced in multiple osteoclasts from several cultures. Scale bar (**A**) 25 μm; (**B**) 50 μm.

and peripheral attachment zone localization of OPN. Importantly, OPN was not detected in the area of the ruffled membrane or on the dentine under the osteoclasts (see Fig. 6A, 45–67 μm sections, and in YZ, XZ scans as shown in Fig. 6B). The surface of the dentine was seen as white spots around the cell in the 40–54 μm scans and these spots were reduced or not seen as the scanning progressed below the dentine surface (58–67 μm).

Transwell Migration Assay

Phagokinesis assays revealed that OPN stimulated motility more effectively than VN, GRGDS peptides. OPN has been shown to be a ligand for CD44 receptor, and anti-OPN and anti-CD44 antibodies inhibited the migration of CD44 transfected fibroblasts toward OPN in Boyden chambers [20]. This strongly suggests CD44-OPN interaction as well as a causative role during chemotactic migration. Therefore, we analyzed CD44 involvement in osteoclast migration by using an antibody to CD44. Transwell and the phagokinetic migration results have demonstrated that OPN stimulated osteoclast motility significantly and antibodies to $\alpha_v\beta_3$, CD44, and OPN blocked chemotactic migration towards OPN (Fig. 7). Even though there is a consistent inhibition of osteoclast migration with the CD44 antibody, the inhi-

bition varies from experiment to experiment due to the specificity of this antibody to chicken cells. As CD44 binds to hyaluronan (HA) with high affinity [31, 32], we studied the effects of OPN alone and OPN/HA together on osteoclast motility. More interestingly, we have shown here that OPN/HA together had greater effects in directing osteoclast migration than OPN or HA alone. The anti-$\alpha_v\beta_3$ antibody partially blocked chemotactic migration towards HA, whereas the inhibition was even greater in the presence of OPN.

Discussion

The data presented here demonstrate that avian osteoclasts secrete OPN from their basolateral cell membranes *in vitro*, but do not secrete at the ruffled border or into the resorption cavities. Addition of soluble OPN to osteoclast cultures mimics the secretion from the basolateral surface, stimulated cell shape changes, and cytoskeletal rearrangement during cell motility. While polarized secretion of OPN from the basolateral surface of the avian osteoclasts supported its characterization as an autocrine motility factor, several investigators have shown that OPN is secreted differently in human osteoclasts, osteoclast-like cells derived from human giant cell tumors of bone (GCT), or rodent osteoclasts [33–35]. These data are compatible with ours except that we were unable to detect OPN in the $\alpha_v\beta_3$ containing focal adhesion sites left by detaching osteoclasts on dentine. We demonstrated that $\alpha_v\beta_3$ ligated with OPN migrates to the adhesion zone of avian osteoclasts and that osteoclast detachment from resorption bays leaves behind $\alpha_v\beta_3$ at the cell attachment sites surrounding the areas of resorption. Dodds et al. have localized OPN at the resorption pits of osteoclasts in bone and have demonstrated that human GCT secretes OPN onto the resorption surfaces of dentine [34]. These results are in agreement with the studies carried out in rodent osteoclasts [35]. We were unable to document this pathway of OPN secretion in avian osteoclasts, and our attempts to improve avian osteoclast pit formation by precoating dentine with OPN were unsuccessful. Precoating may not have been sufficient to provide strong anchoring during the excavation of a deep resorption pit. We were able to document this pathway of OPN secretion into resorption bays of osteoclasts isolated from mice [30]. Thus, the OPN secretary pathway demonstrates a variation across different species. The significance of the lack of secretion by the avian osteoclast into the resorption may explain the shallow and superficial nature of the pits generated by avian osteoclasts.

Migration of cells is brought about by the changes in cytoskeletal organization, cell shape, and adhesion. Actin cytoskeleton undergoes many different transformations as the cell moves forward. The migratory osteoclasts (Figs. 2 and 3) have demonstrated extension of lamellipodia at the leading edge of the cell. The formation of new podosome structures at the membrane protrusion stabilizes the contact with the substratum as well as provides a driving force to pull the cell forward. Membrane protrusions and the formation of new adhesive contacts at the leading edge of a migrating cell must be coordinated with down regulation of adhesion and retraction site at the trailing end of the cell [19, 36]. Osteoclasts exhibit different phenotypic changes (Figs. 2 and 3) during migration as they move forward. The dendritic structure of the motile osteoclast in Figure 3 may be due to the stretching of the actin cortex to move the cell forward. This cycle may already have occurred in osteoclast shown in Figure 2B. Therefore, it is possible that the differences in the cell shape in Figures 2 and 3 may be due to the fact that these osteoclasts are at the different phases of cell migration cycle [37].

It has been shown that the integrin family of cell surface receptors not only mediates cell adhesion but also is directly involved in cell migration [38, 39]. Blocking studies using antibodies and competitive ligands have demonstrated that the $\alpha_v\beta_3$ integrin is essential for bone attachment and resorption *in vitro* [40, 41]. We examined the localization of integrin $\alpha_v\beta_3$ in adherent and migrating osteoclasts on dentine slices. Osteoclasts expressed the $\alpha_v\beta_3$ integrin on the basolateral membrane, in agreement with the data of Lakkakorpi et al. [42], and in the clear zone [43] of the resorbing osteoclasts. Migrating osteoclasts demonstrated colocalization of actin and $\alpha_v\beta_3$ integrins at the adhesion site.

CD44 is an integral membrane glycoprotein and is a transmembrane receptor for several extracellular matrix elements such as hyaluronate [44, 45], OPN [20], collagen type 1, and fibronectin [46]. OPN binds to extracellular domain of CD44 and mediates chemotactic migration [47, 48]. Zohar et al. [49] have demonstrated perimembranous distribution of OPN which colocalizes with CD44 and ERM proteins in migrating embryonic fibroblast cells, activated macrophages, and metastatic breast cancer cells.

CD44 was first identified as hyaluronan (HA) receptor, and clustering of CD44 on the cell surface has been proposed as a possible mechanism of modulating the HA binding function of CD44 [31]. Even though OPN/HA together had greater effects in directing osteoclast migration, HA alone did not have any effect on bone resorption activity of osteoclast (unpublished observation). One potential reason could be that addition of both HA and OPN extracellularly increases the avidity of OPN binding to CD44 receptor. Also, HA binding to CD44 is dependent on CD44 activation. CD44 activation by OPN/$\alpha_v\beta_3$ signaling may increase its binding to HA.

Our results demonstrate that $\alpha_v\beta_3$ and CD44 receptors are capable of interacting with OPN. OPN and HA are capable of interacting with CD44 receptor. In ad-

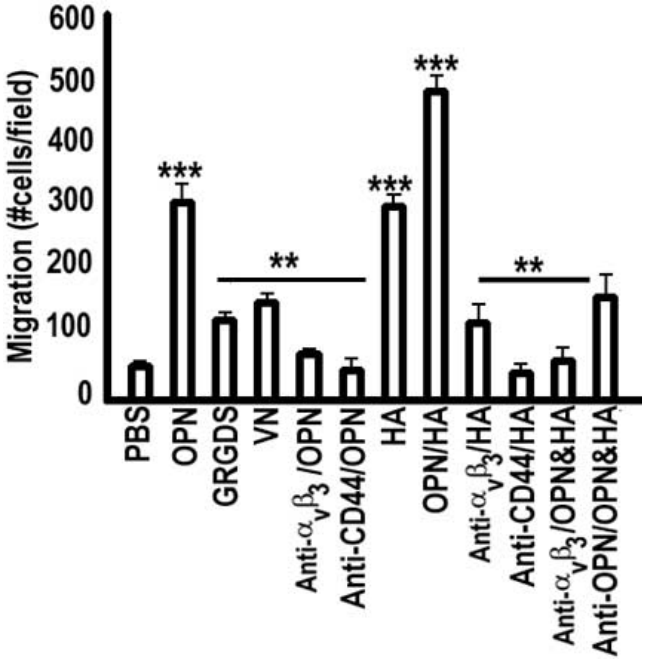

Fig. 7. Transwell migration assay. Effect of OPN on chemotactic migration of osteoclasts. Chemotaxis assays were performed in a transwell chamber. The test substrates such as GRGDS, vitronectin (VN), osteopontin (OPN), and hyaluronic acid (HA) were added to the bottom wells. The indicated antibodies were added to the cells in the upper chamber and migration was done for 12–14 hours. Cells that migrated to the undersides were stained, visualized, and counted. Data are presented as the number of cells migrated. Results shown are mean ± SEM of three independent experiments. ***P0.0001-OPN, OPN/HA, HA vs PBS, GRGDS, and VN; **P0.001-GRGDS, VN vs PBS; **P0.001-anti-$\alpha_v\beta_3$/OPN; anti-CD44/OPN; anti-CD44/HA; anti-$\alpha_v\beta_3$/HA; anti-OPN/OPN & HA, anti-$\alpha_v\beta_3$/HA & OPN vs OPN or HA.

dition to that, the migratory effects of osteoclasts are mediated through both $\alpha_v\beta_3$ and CD44 receptors and there is a cooperativity between these two receptors. OPN-mediated osteoclast motility and bone resorption require both $\alpha_v\beta_3$ and CD44 receptors. Our recent observations have demonstrated that osteoclasts from OPN null mice are hypomotile, less resorptive, and showed significantly decreased levels of CD44 expression at the basolateral surface, whereas the surface expression of integrin $\alpha_v\beta_3$ remains the same in both wild type and OPN null osteoclasts [30]. This observation demonstrates that CD44 receptor has unique functions in osteoclast motility. We cannot exclude the possibility that $\alpha_v\beta_3$-initiated signaling mechanism is crucial and central to the migratory processes and CD44 expression as well as CD44 signaling cascade relies on $\alpha_v\beta_3$-initiated pathways.

Acknowledgments. This work was supported by National Institutes of Health Grants AR46292 (to M.A.C), AR 41677 (to K.A.H) and DK 09976 (to K.A.H). We thank Dr. David Cheresh (Scripps Research Institute, LaJolla, USA) for the antibody to integrin $\alpha_v\beta_3$; Dr. L. Gerstenfeld (Harvard University Boston, Massachusetts) for the antibody to chicken OPN; Dr. John Freeman (Department of Orthopedics, Barnes-Jewish Hospital, St. Louis, MO) for assistance with the confocal microscopy; Dr. Arasu Chellaiah for proof reading the manuscript and Kathy Jones for secretarial assistance.

References

1. Kanehisa J, Heersche JNM (1988) Osteoclastic bone resorption: in vitro analysis of the rate of resorption and migration of individual osteoclasts. Bone 9:73–79
2. Zambonin-Zallone A, Teti A, Grano M, Rubinacci A, Abbadini M, Gaboli M, Marchisio C (1989) Immunocytochemical distribution of extracellular matrix receptors in human osteoclasts: a beta3 integrin is co-localized with vinculin and talin in the podosomes of osteoclastoma giant cells. Exp Cell Res 182:645–652
3. Roodman GD (1999) Cell biology of the osteoclast. Exp Hematol 27:1229–1241
4. Zambonin-Zallone A, Teti A, Carano A, Marchisio PC (1988) The distribution of podosomes in osteoclasts cultured on bone laminae: effect of retinol. J Bone Miner Res 3:517–523
5. Lakkakorpi PT, Vaananen HK (1991) Kinetics of the osteoclast cytoskeleton during the resorption cycle in vitro. J Bone Miner Res 6:817–826
6. Marchisio PC, Cirillo D, Teti A, Zambonin Zallone A, Tarone G (1987) Rous sarcoma virus-transformed fibroblasts and cells of monocytic origin display a peculiar dot-like organization of cytoskeletal proteins involved in microfilament-membrane interaction. Exp Cell Res 169: 202–214
7. Holtrop ME, King GJ (1977) The ultra structure of osteoclast and its functional implications. Clin Orthop 123:177–196
8. Helfrich MH, Nesbitt SA, Dorey EL, Horton MA (1992) Rat osteoclasts adhere to a wide range of RGD (Arg-Gly-Asp) peptide-containing proteins, including the bone sialoproteins and fibronectin, via a B_3 integrin. J Bone Miner Res 7:335–343
9. Ross FP, Chappel J, Alvarez JI, Sander D, Butler WT, Farach-Carson MC, Mintz KA, Robey PG, Teitelbaum DA, Cheresh DA (1993) Interactions between the bone matrix proteins osteopontin and bone sialoprotein and the osteoclast integrin alpha(v)beta(3) potentiate bone resorption. J Biol Chem 268:9901
10. Flores ME, Norgard M, Heinegard D, Reinholt FP, Andersson G (1992) RGD-directed attachment of isolated rat osteoclasts to osteopontin, bone sialoprotein, and fibronectin. Exp Cell Res 201:526–530
11. Denhardt DT, Guo X (1993) Osteopontin: a protein with diverse functions. FASEB J 7:1475–1482
12. Sodek J, Chen J, Kasugai S, Nagata T, Zhang Q, McKee A, Nanci A (1992) Elucidating the functions of bone sialoprotein and osteopontin in bone formation. In: Price HS (ed) Chemistry and biology of mineralized tissues. Elsevier Science Publishers, New York, pp 97–306
13. Gerstenfeld LC, Uporova T, Ashkar S, Salih E, Gotoh Y, McKee MD, Nanci A, Glimcher MJ (1995) Regulation of avian osteopontin pre-and posttranscriptional expression in skeletal tissues. Ann NY Acad Sci 760:67–82
14. Ikeda T, Nomura S, Yamaguchi A, Suda T, Yoshiki S (1992) In situ hydridization of bone matrix proteins in undecalcified adult rat bone sections. J Histochem Cytochem 40:1079–1088
15. Chellaiah M, Hruska KA (1996) Osteopontin stimulates gelsolin associated phosphoinositide levels and PtdIns 3-hydroxyl kinase. Mol Biol Cell 7:743–753
16. Hruska KA, Rolnick F, Huskey M, Alvarez U, Cheresh D (1995) Engagement of the osteoclast integrin alpha$_v$beta$_3$ by osteopontin stimulates phosphatidylinositol 3-hydroxyl kinase activity. Endocrinology 136:2984–2992

17. Chellaiah M, Fitzgerald C, Alvarez U, Hruska K (1998) C-*src* is required for stimulation of gelsolin-associated PI3-K. J Biol Chem 273:11908–11916
18. Chellaiah M, Biswas RS, Yuen D, Alvarez UM, Hruska K (2001) Phosphoinositol 3,4,5-trisphosphate directs association of SH2 containing signaling proteins with gelsolin. J Biol Chem 276:47434–47444
19. Lauffenburger DA, Horwitz AF (1996) Cell migration: a physically integrated molecular process. Cell 84:359–369
20. Weber GF, Ashkar S, Glimcher MJ, Cantor H (1996) Receptor-ligand interaction between CD44 and osteopontin (Eta-1) Science 271:509–512
21. Udagawa N, Findlay DM, Martin TJ (1996) CD44 involvement in osteoclast differentiation as well as bone resorption by mature osteoclasts. J Bone Miner 11:S112
22. Gupta A, Edwards JC, Hruska KA (1996) Cellular distribution and regulation of NHE-1 isoform of the Na-H exchanger in the avian osteoclast. Bone 18:87–95
23. Chellaiah M, Kizer N, Silva M, Alvarez U, Kwiatkowski KA, Hruska KA (2000) Gelsolin deficiency blocks podosome assembly and produces increased bone mass and strength. J Cell Biol 148:665–678
24. Chellaiah M, Hruska K (1998) Osteopontin (Review) J Drug News Perspect 11:350–355
25. Takaishi K, Sasaki T, Taka L (1995) Cell motility assay and inhibition by Rho-GDP dissociation inhibitor. Meth Enzymol 256:336–347
26. Chellaiah M, Soga N, Swanson S, McAllister S, Alvarez D, Wang D, Dowdy SF, Hruska KA (2000) Rho-A is critical for osteoclast podosome organization, motility, and bone resorption. J Biol Chem 275:11993–12002
27. Orlando R, Cheresh DA (1991) Arginine-glycine-aspartic acid binding leading to molecular stabilization between integrin avb_3 and its ligand. J Biol Chem 266:19543–19550
28. Liaw L, Skinner MP, Raines EW, Ross R, Cheresh DA, Schwartz SM, Giachelli CM (1995) The adhesive and migratory effects of osteopontin are mediated via distinct cell surface integrins. Role of a_vb_3 in smooth muscle cell migration to osteopontin *in vitro*. J Clin Invest 95:713–724
29. Clyman RI, Mauray F, Kramer RH (1992) b1 and b3 integrins have different roles in the adhesion and migration of vascular smooth muscle cells on extracellular matrix. Exp Cell Res 200:272–284
30. Chellaiah M, Alvarez U, Strauss-Schoenberger J, Rifas L, Rittling S, Denhardt D, Hruska K (2002) Osteopontin deficiency produces osteoclast dysfunction due to reduced CD44 surface expression. Mol Biol Cell (in press)
31. Lesley J, Hascall VC, Tammi M, Hyman R (2000) Hyaluronan binding by cell surface CD44. J Biol Chem 275:26967–26975
32. Herrlich P, Zoller M, Pals ST, Ponta H (1993) CD44 splice variants: metastases meet lymphocytes. Immunol Today 14:395–399
33. Chenu C, Colucci S, Grano M, Zigrino P, Barattolo R, Zambonin G, Baldini N, Vergnaud P, Delmas PD, Zallone AZ (1994) Osteocalcin induces chemotaxis, secretion of matrix proteins, and calcium-mediated intracellular signaling in human osteoclast-like cells. J Cell Biol 127:1149–1158
34. Dodds RA, Connor JR, James IE, Rykaczewski EL, Appelbaum E, Dul E, Gowen M (1995) Human osteoclasts, not osteoblasts, deposit osteopontin onto resorption surfaces: an in vitro and ex vivo study of remodeling bone. J Bone Miner Res 10:1666–1680
35. Maeda M, Kukita T, Akamine A, Kukita A, Iijima T (1994) Localization of osteopontin in resorption lacunae formed by osteoclast-like cells: a study by a novel monoclonal antibody which recognizes rat osteopontin. Histochemistry 102:247–254
36. Worthylake RA, Burridge K (2001) Leukocyte transendothelial migration: orchestrating the underlying molecular machinery. Curr Opin Cell Biol 13:569–577
37. Alberts B, Bray D, Lewis J, Raff M, Roberts K, Watson JD (1994) The cytoskeleton.Molecular biology of the cell, 3rd ed. Garland Publishing, Inc., New York, London, pp 828–847
38. Leavesley DI, Ferguson GD, Wayner EA, Cheresh DA (1992) Requirement of the integrin $beta_3$ subunit for carcinoma cell spreading or migration on vitronectin and fibrinogen. J Cell Biol 117:1101–1109
39. Akiyama H, Akiyama SK, Yamada S, Chen WT, Yamada KM (1989) Analysis of fibronectin receptor function with monoclonal antibodies: roles in cell adhesion, migration, matrix assembly, and cytoskeletal organization. J Cell Biol 109:863–875
40. Engleman VW, Nickols GA, Ross FP, Horton MA, Griggs DW, Settle SL, Ruminski PG, Teitelbaum SL (1997) A peptidomimetic antagonist of the alpha (v) beta (3) integrin inhibits bone resorption in vitro and prevents osteoporosis in vivo. J Clin Invest 99:2284–2292
41. Carron CP, Meyer DM, Engleman VW, Rico JG, Ruminski PG, Ornberg RL, Westlin WF, Nickols GA (2000) Peptidomimetic antagonists of alphavbeta3 inhibit bone resorption by inhibiting osteoclast bone resorptive activity, not osteoclast adhesion to bone. J Endocrinol 165:587–598
42. Lakkakorpi PT, Helfrich MH, Horton MA, Vaananen HK (1993) Spatial organization of microfilaments and vitronectin receptor, alpha (v) beta (3), in osteoclasts. J Cell Sci 104:663–670
43. Nakamura I, Pilkington MF, Lakkakorpi PT, Lipfert L, Sims SM, Dixon SJ, Rodan GA, Duong LT (1999) Role of alpha (v) beta (3) integrin in osteoclast migration and formation of the sealing zone. J Cell Sci 112(22):3985–3993
44. Miyake K, Underbill CB, Lesley J, Kincade PW (1990) Hyaluronate can function as a cell adhesion molecule and CD44 participates in hyaluronate recognition. J Exp Med 172:69–75
45. Lesley J, He Q, Miyake K, Hamann A, Hyman R, Kincade PW (1992) Requirements for hyaluronic acid binding by CD44: a role for the cytoplasmic domain and activation by antibody. J Exp Med 175:257–266
46. Rudzki Z, Jothy S (1997) CD44 and the adhesion of neoplastic cells. J Clin Pathol:Mol Pathol 50:57–71
47. Weber GF, Ashkar S, Cantor H (1991) Interaction between CD44 and osteopontin as a potential basis for metastasis formation. Proc Assoc Am Physicians 109:1–9
48. Katagiri YU, Sleeman J, Fujii H, Herrlich P, Hotta H, Tanaka K, Chikuma S, Yagita H, Okumura K, Murakami I, Saiki I, Chambers AF, Uede T (1999) CD44 variants but not CD44s cooperate with b1-containing integrins to permit cells to bind to osteopontin independently of arginine-glycine-aspartic acid, thereby stimulating cell motility and chemotaxis. Cancer Res 59:219–226
49. Zohar R, Suzuki N, Suzuki K, Arora P, Glogauer M, McCulloch CA, Sodek J (2000) Intracellular osteopontin is an integral component of the CD44-ERM complex involved in cell migration. J Cell Physiol 184:118–130